

# Galaxy clustering and dark energy

Dipak Munshi,<sup>1,2★</sup> Cristiano Porciani<sup>1,3</sup> and Yun Wang<sup>4</sup>

<sup>1</sup>*Institute of Astronomy, Madingley Road, Cambridge CB3 0HA*

<sup>2</sup>*Astrophysics Group, Cavendish Laboratory, Madingley Road, Cambridge CB3 0HE*

<sup>3</sup>*Institute of Astronomy, Department of Physics, ETH Hönggerberg, 8093 Zürich, Switzerland*

<sup>4</sup>*Department of Physics and Astronomy, University of Oklahoma, Norman, OK 73019, USA*

Accepted 2003 December 1. Received 2003 December 1; in original form 2003 February 21

## ABSTRACT

We study the evolution of galaxy clustering in various cosmological models with quintessence. We investigate how the analytical predictions vary with the change of the dark energy equation of state  $w_X$ . Comparing these predictions against available data, we discuss to what extent the problems of galaxy biasing can be modelled. This will be key in constraining the dark energy equation of state with future galaxy surveys. We use a compilation of various surveys to study the number density and amplitude of galaxy clustering from observations of the local universe at  $z \sim 0$  to that of the Lyman-break galaxies and Ly  $\alpha$  emitters at  $z \sim 4.9$ . We find that there is a degeneracy between the dark energy equation of state and the way galaxies populate dark matter haloes; objects are more biased in models with more negative values of dark energy equation of state  $w_X$ .

We conclude that, while future all-sky cosmic microwave background observations will determine cosmological parameters with unprecedented precision, and cross-correlation of weak lensing experiments and galaxy surveys will provide a cleaner and more accurate picture of bias associated with collapsed objects, the rate of growth of large-scale structure in such surveys can potentially constrain the equation of state of dark energy and the potential of the scalar field associated with quintessence. In particular, we show that the abundance and spatial distribution of galaxy clusters at intermediate redshifts strongly depend on the dark energy equation of state. When accurate measurement of galaxy clustering at high redshift becomes possible, it will provide constraints on dark energy that are independent and complementary to Type Ia supernova studies.

**Key words:** methods: analytical – methods: numerical – methods: statistical – galaxies: clusters: general – cosmology: theory.

## 1 INTRODUCTION

It is generally believed that small perturbations in the matter density, generated by quantum effects during inflation, eventually grow due to gravitational instability, and finally collapse to produce luminous objects such as galaxies and clusters which can be observed today. The evolution of galaxy clustering can be used to constrain cosmological models and the dark matter scenarios. In particular, the evolution of clustering with redshift can put direct constraints on models for the evolution of density perturbations. In this paper we study how the equation of state of dark energy affects the observed clustering of luminous objects.

For many years the study of the spatial distribution of galaxies at high redshift has been rather sketchy and affected by various ob-

servational limitations. Early studies showed that galaxy clustering, when parametrized by the rms amplitude of fluctuations in the galaxy counts within a fixed comoving scale, typically decreases with redshift for moderately deep samples ( $0 < z \lesssim 1$ ). Recent progress in colour selection criteria has made empirical studies of the high-redshift universe possible observationally. Colour selection such as the Lyman-break technique (Steidel et al. 1996, 1998; Madau et al. 1996; Lowenthal et al. 1997) or the photometric redshift technique (see, for example, Wang, Bahcall & Turner 1998; Budavári et al. 2000; Fernández-Soto et al. 2001), allows us to efficiently identify classes of galaxies in a pre-assigned redshift range based on their spectral energy distribution. This has resulted in the compilation of large and well-controlled samples of galaxies at  $z > 2$  which are suitable for clustering studies (see, for example, Porciani & Giavalisco 2002 and references therein, for details). These studies measured a very strong clustering amplitude, comparable to that of present-day galaxies. It is worth stressing, however, that Lyman-break galaxies

★E-mail: munshi@ast.cam.ac.uk

(LBG hereafter) essentially consist of actively star-forming galaxies; in comparison, quiescent galaxies at high redshifts are much less efficiently identified with current instrumentation.

Although the detection of strong clustering seems to be quite robust at high redshift, the current samples still contain too few objects and cover too small an area on the sky to accurately measure the corresponding correlation functions. The signal-to-noise ratio of the current measurements is of the order of 3 for the two-point statistics, and the dispersion among different measurements suggests the possibility of systematic errors (Porciani & Giallisco 2002). Robust statistical techniques combined with next generation extensive surveys can greatly enhance our knowledge of clustering of high-redshift galaxies, allowing us to use it as a test for cosmological scenarios.

A number of clustering analyses are presently available for galaxies at  $z \lesssim 5$ . Various factors, such as scale dependence, type selection and Malmquist bias, need, however, to be taken into account to compare the outcome of different studies (see, for example, Magliocchetti et al. 2000). In fact, the clustering properties of galaxies are scale-dependent and surveys sample a variety of different scales. Moreover, it is well known that galaxy clustering depends on a series of characteristics of the galaxy population under scrutiny (e.g. morphological type, colour, star formation rate) and surveys generally use different criteria to select the objects they study. Finally, Malmquist bias is due to the fact that within a given survey more distant galaxies tend to have brighter absolute magnitude and will, in general, not have the same clustering amplitude. All these effects will have to be taken into account while we compare theoretical prediction from various cosmologies with observational data.

Weak lensing surveys have also started to make progress in mapping directly the three-dimensional dark matter distribution in the universe. In the near future, such surveys will not only study the statistical nature of clustering, but will also measure the detailed features of the underlying mass distribution. Cross-correlating weak lensing maps with galaxy surveys will provide us with a unique way to probe gravitational clustering, and hence the nature of bias associated with the luminous objects. Therefore, it is important to see how varying the equation of state in quintessence cosmologies can affect the nature of clustering of dark haloes and galaxies.

The main uncertainty in comparing theoretical predictions about growth of gravitational instability and observational data of galaxy clustering originates from the fact that galaxies might be biased tracers of the underlying mass distribution. In fact, it is well known that different galaxy populations (selected by morphological type, luminosity, star formation rate) cluster differently, hence not all of them can trace the underlying mass distribution. A number of models (based on analytical reasoning or numerical simulations) are available to quantify the expected degree of biasing associated with galaxies and clusters (see, for example, Magliocchetti & Porciani 2003 and references therein). Most of them associate luminous objects with their hosting dark matter haloes. A general prediction is that the clustering amplitude of the most massive haloes at any given epoch is amplified with respect to that of the mass distribution, while very small haloes are nearly good tracers of the mass-density field (e.g. Mo & White 1996; Catelan et al. 1998; Porciani et al. 1998; Coles, Melott & Munshi 1999). Not surprisingly such models are too simplistic to encompass all the detailed information and the non-linear physics necessary to understand the formation and clustering of galaxies. In spite of this, they are able to make reliable predictions of the expected amplitude of galaxy clustering. In general, the

strong clustering of high-redshift galaxies has been regarded as an indication of the overall robustness of the theory and as evidence for the reality of galaxy biasing.

Recent cosmological observations favour an accelerating universe (Garnavich et al. 1998a; Riess et al. 1998; Perlmutter et al. 1999). This implies the existence of energy of unknown nature (dark energy), which has negative pressure. Various observations are consistent with dark energy being a non-zero cosmological constant (see, for example, Wang & Garnavich 2001; Bean & Melchiorri 2002). However, many other alternative dark energy candidates have been considered, and are consistent with data as well. For example, quintessence, k-essence, spintessence, etc. (Freese et al. 1987; Peebles & Ratra 1988; Frieman et al. 1995; Caldwell, Dave & Steinhardt 1998; Garnavich et al. 1998b; White 1998; Efstathiou 1999; Steinhardt, Wang & Zlatev 1999; Podariu & Ratra 2000; Sahni & Wang 2000; Sahni & Starobinsky 2000; Saini et al. 2000; Waga & Frieman 2000; Huterer & Turner 2001; Ng & Wiltshire 2001; Podariu, Nugent & Ratra 2001; Sarbu, Rusin & Ma 2001; Weller & Albrecht 2002).

Various dark energy models can be conveniently classified according to the equation of state of the dark energy component,  $w_X$ . For example, for quintessence models,  $dw_X/dz > 0$ , while for k-essence models,  $dw_X/dz < 0$ . However, it is extremely difficult to determine the time dependence of  $w_X(z)$  (Maor, Brustein & Steinhardt 2001; Barger & Marfatia 2001; Maor et al. 2002). Wang & Garnavich (2001) have shown that it is more optimal to constrain the time dependence of the dark energy density  $\rho_X(z)$ , instead of  $w_X(z)$ . In this paper, we only consider toy models with  $w_X = \text{constant}$  for simplicity and illustration. This is appropriate for our purposes, because current galaxy clustering data cannot place useful constraints on the time dependence of  $w_X(z)$ . However, our method can readily be extended to models with a time-dependent equation of state. Our results will also have direct relevance for programs which focus on reconstructing the potential energy  $V(\phi)$  of the quintessence field from observed galaxy clustering data.

There are many other probes of dark energy. These include the distance-redshift relations of cosmological standard candles, cosmic microwave background (CMB) anisotropy, volume-redshift test using galaxy counts, the evolution of galaxy clustering, weak lensing, etc. These different methods to probe dark energy are complementary to each other, and can provide important consistency checks, due to the different sources of systematics in each method (see, for example, Kujat et al. 2002, and references within).

## 2 EVOLUTION OF CLUSTERING IN QUINTESSENCE COSMOLOGIES

Hamilton et al. (1991) proposed a scaling ansatz for computing the non-linear matter power spectrum of a given cosmological model at any epoch. This method was later extended by various authors to reproduce the outcome of high-resolution numerical simulation in a cold dark matter (CDM) scenario (see, for example, Peacock & Dodds 1996; Smith et al. 2003). In the version by Peacock & Dodds (1996) that we adopt here, this ansatz essentially consists of postulating that  $4\pi k^3 P(k) = f[4\pi k_1^3 P_1(k_1)]$ , where  $P(k)$  is the non-linear power spectrum,  $P_1$  is the linear power spectrum, and the function  $f$  in general will depend on the initial power spectra. The linear power spectrum is evaluated at a different wavenumber,  $k_1 = [1 + 4\pi k^3 P(k)]^{-1/3} k$ , hence the mapping is non-local in nature. The form of the function  $f$  is calibrated against  $N$ -body simulations, by

assuming that it matches the predictions of linear theory on large scales, and of stable clustering on small scales (see Smith et al. 2003 for a critical discussion). Ma et al. (1999) showed that, at  $z = 0$ , the formula of Peacock & Dodds (1996) is accurate even in the presence of quintessence. However, at earlier epochs, it tends to underestimate the non-linear power on scales smaller than  $\sim 1 h^{-1}$  Mpc by up to 30 per cent. Given that we are interested in galaxy clustering on mildly non-linear scales (and given the uncertainties on present-day determinations of galaxy clustering at high  $z$ ), the formulation of Peacock & Dodds is good enough for our analysis.

The cosmological model enters the scaling ansatz primarily through the linear growth function  $D(z)$ ,<sup>1</sup> so that  $P_1(k, z) = [D(z)/D(z=0)]^2 P_1(k, z=0)$ . The linear growth function is evaluated directly from

$$\ddot{D}(z) + 2H(z)\dot{D}(z) - \frac{3}{2}H_0^2\Omega_m(1+z)^3D(z) = 0, \quad (1)$$

where the dots denote derivatives with respect to  $t$ . For a constant dark energy equation of state  $w_X$ , the evolution of the Hubble parameter  $H(z)$  can be written as

$$H(z) = H_0[\Omega_m(1+z)^3 + (1 - \Omega_m - \Omega_X)(1+z)^2 + \Omega_X(1+z)^{3(1+w_X)}]^{1/2}. \quad (2)$$

In general, equation (1) must be solved numerically because the usual integral equation for  $D(z)$  (Heath 1977) does not hold in the presence of quintessence (unless  $w = -1$  or  $w = -1/3$ ). However, when  $\Omega_m + \Omega_X = 1$  and  $w = \text{constant}$ , equation (1) can be solved analytically in terms of hypergeometric functions (Padmanabhan 2003). Useful approximations for the linear growth functions can be found in Lahav et al. (1991) for  $\Lambda$ CDM models and in Wang & Steinhardt (1998) for QCDM models. See Benabed & Bernardeau (2001) for more on power spectrum evolution in quintessence cosmologies.

In this paper, we assume that the matter density parameter  $\Omega_m = 0.3$ , the dark energy density parameter  $\Omega_X = 0.7$ , the Hubble constant  $H_0 = h \, 100 \, \text{km s}^{-1} \text{Mpc}^{-1}$  with  $h = 0.7$ , and the rms density fluctuation within a top-hat sphere of radius  $8 h^{-1}$  Mpc linearly extrapolated to today  $\sigma_8 = 0.8$ . The four quintessence models we have studied are  $w_X = -1/3, 2/3, -1, -1.9$ .  $w_X = -1.9$  is taken as an example of the class of models which violate the weak energy condition (WEC; Wald 1984) of recent theoretical interest (Caldwell 2002; Frampton 2003; Onemli & Woodard 2002).

To see how the evolution of clustering varies in quintessence models, we calculate the rms fluctuation  $\sigma_8(z)$  as follows

$$\sigma_8^2(z) = \int_0^\infty \frac{dk}{k} \Delta_1^2(k, z) \left( \frac{3j_1(kr)}{kr} \right)^2, \quad (3)$$

where  $\Delta_1^2(k, z) = 4\pi k^3 P_1(k, z)$ , and  $r = 8 h^{-1}$  Mpc. We can similarly define the rms fluctuation in galaxy density as  $\sigma_8^{(g)}(z)$ . It is sometimes convenient to relate the mass and galaxy fluctuations on the  $8 h^{-1}$  Mpc scale by introducing the bias parameter  $b_8(z) = \sigma_8^{(g)}(z)/\sigma_8(z)$ .

Fig. 1 shows analytical computations of  $\sigma_8$  (and  $\sigma_8^{(g)}$ ) as a function of redshift  $z$  for various quintessence models, together with observational data. Except for four new data points for LBG at  $z = 3$  (Porciani & Giavalisco 2002; Adelberger et al. 2003),  $z = 4$  (Ouchi et al. 2001), and for Ly  $\alpha$  emitters at  $z = 4.86$  (Ouchi et al. 2003), the observational data for  $\sigma_8^{(g)}(z)$  are from Magliocchetti et al. (2000), converted to each model as described in their paper (see Appendix

A). The solid lines represent the linear growth rate  $D(z)$  (normalized so that  $D \rightarrow (1+z)^{-1}$  when  $z \rightarrow \infty$ ) for various cosmologies as a function of redshift. The short-dashed lines represent the theoretical  $\sigma_8(z)$ ; the two dashed lines are normalized to Automated Plate Measuring (APM) and *IRAS* surveys at low redshift, respectively. The general trend (masked by large error bars) is that  $\sigma_8^{(g)}$  decreases between  $z = 0$  and  $z = 2$ , while it either remains constant or increases at higher redshifts. A similar behaviour is seen in numerical simulations for the clustering of dark matter haloes (see, for example, Jenkins et al. 1998). Note that the most recent data sets correspond to substantially smaller error bars at high  $z$ . However, it is important to stress that Ouchi et al. (2001, 2003) have assumed that the slope of the correlation function is  $\gamma = 1.8$ , so that the corresponding error bars for  $\sigma_8^{(g)}(z)$  are underestimated (not including the uncertainty in  $\gamma$ ).

It is clear that current clustering data are not very constraining on the dark energy equation of state  $w_X$ , mainly because the scatter of the data points is large in Fig. 1. However, because different types of galaxies are expected to cluster differently, in the next section we will try to reduce this scatter by dividing the galaxies into subgroups.

### 3 CLUSTERING OF GALAXIES AND DARK MATTER HALOES IN QUINTESSENCE COSMOLOGIES

In general, it is not clear how the spatial distribution of galaxies is related to the underlying mass distribution; this relationship is likely to be non-linear, non-local, scale-dependent, type-dependent and even stochastic (Catelan et al. 1998; Dekel & Lahav 1999). However, due to the lack of the complete picture of how galaxies are formed, various analytical and semi-analytical models have been proposed which capture some basic flavours of galaxy clustering.

We parametrize the clustering properties of a population of cosmic objects through a bias parameter  $b$  (a function of separation and redshift) defined by the ratio between the galaxy autocorrelation function,  $\xi_g$ , and the corresponding quantity for the mass density distribution,  $\xi$ , as

$$b^2(r, z) = \xi_g(r, z)/\xi(r, z). \quad (4)$$

In what follows the scale dependence will be neglected because we will either consider the large separation limit (for the models) or refer to a limited range of separations accessible to a given survey (for the data) over which only small variations of the bias parameter are possible.

#### 3.1 No merger or galaxy conserving model

We first consider a simple biasing scheme which treats galaxies as test particles moving in the overall potential generated by the large-scale structure. It assumes that a galaxy population is generated at a given cosmic epoch with a density distribution which is linked to the mass density by a linear bias parameter. In other words, test particles representing galaxies are distributed throughout the Universe in such a way that their density contrast is directly proportional to the density contrast of the underlying mass distribution. This model also assumes that these test particles follow the cosmic flow. The conservation of galaxy number density then is used to compute the evolution of bias associated with these particles. It can be shown that the evolution of this test particle bias can be written as

$$b(z) = 1 + [b(z_*) - 1] \frac{D(z_*)}{D(z)} = 1 + (b_0 - 1) \frac{D(z=0)}{D(z)}, \quad (5)$$

<sup>1</sup> The matter transfer function has negligible dependence on dark energy models on the scales of interest to us Ma et al. (1999).

## All Galaxies

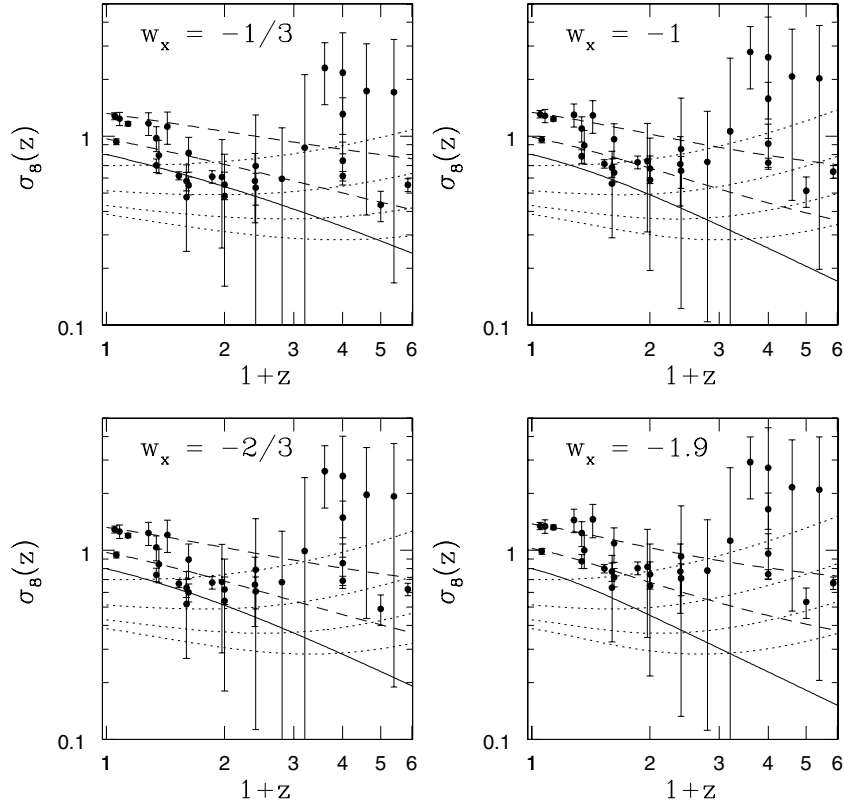


**Figure 1.** Analytical computations of  $\sigma_8$  and  $\sigma_8^{(g)}$  as a function of redshift  $z$  for various quintessence models are compared with observational results. The solid lines represent the linear growth rate  $D(z)$  for various cosmologies as a function of redshift. The short-dashed lines represent the theoretical  $\sigma_8(z)$ ; the two dashed lines are normalized to APM and *IRAS* surveys at low redshift, respectively. The dotted lines represent the predictions from the halo model. We use the analytical results of Mo & White (1996) to compute the bias parameter for haloes larger than a given mass threshold. Curves from the bottom upwards correspond to haloes with masses greater than  $10^9$ ,  $10^{10}$ ,  $10^{11}$  and  $10^{12} M_\odot$ . The various data sets consist of large galaxy surveys at low redshift such as *IRAS* and APM, and smaller surveys covering less survey area at high redshift. It is clear that current clustering data are not very constraining on the dark energy equation of state  $w_X$ , although there seems to be some evidence that  $w_X < -2/3$  may be favoured.

where  $D(z)$  is the linear growth rate for gravitational clustering which typically depends on the background dynamics of the Universe,  $z_*$  denotes the epoch of ‘galaxy formation’, and  $b_0$  is the bias at the present epoch. This can be understood as follows. If we assume a certain class of galaxies is formed at a particular redshift due to a specific gas-dynamical formation mechanism, it will carry a specific bias tag, which one can argue is largely independent of the local environment and hence constant for a specific galaxy type. However, once formed, these galaxies will have to move due to the gravitational field. The final expression for the galaxy bias is derived by assuming constant comoving number density for these galaxies (Dekel 1986; Fry 1986; Dekel & Rees 1987; Nusser & Davis 1994). This model is also known as the galaxy conserving model (Matarrese et al. 1997). However, we should keep in mind that the basic assumption of inert indestructible nature of galaxies is not correct.

In Figs 2–4 we plot the test-particle bias parameters (dashed lines) associated with various models with quintessence and compare them against survey results. Corresponding values for  $\sigma_8$  are displayed in Fig. 1 (short-dashed lines). In Figs 2–4 we have divided the observed galaxy population into three subsamples. It is known from earlier studies that various types of galaxies cluster differently. Comparing samples which are inherently similar, such as red galaxies or galax-

ies with strong star formation rates, does tend to reduce the scatter found among the clustering properties extracted from different surveys.

Note that in Fig. 1 we have compared the observed results against the theoretical predictions by forcing the galaxy clustering predictions to match low-redshift results from the APM and *IRAS* surveys respectively; on the other hand, in Figs 2–4, the theoretical bias predictions were normalized to different values extracted from various subsamples of the APM galaxies with similar characteristics.

All the observational data in Figs 2–4 are from Magliocchetti et al. (2000), except for the four new data points in Fig. 4, which are for LBG at  $z = 3$  (Porciani & Gialalisco 2002; Adelberger et al. 2003),  $z = 4$  (Ouchi et al. 2001), and Ly  $\alpha$  emitters at  $z = 4.86$  Ouchi et al. (2003). Once again, we stress that these four new data points have substantially smaller error bars. However, Ouchi et al. (2001, 2003) assumed  $\gamma = 1.8$ , hence the error bars for  $b(\bar{r}, z)$  are underestimated (not including the uncertainty in  $\gamma$ ).

Note that the scatter of the data points in Fig. 4 is much larger than in Figs 2 and 3, and there are two sets of dashed curves representing the test-particle model in Fig. 4. One set of dashed curves is anchored at low redshift to the Stromlo–APM survey (only starburst galaxies), while the other set of dashed curves is anchored to LBG at  $z = 3$ .

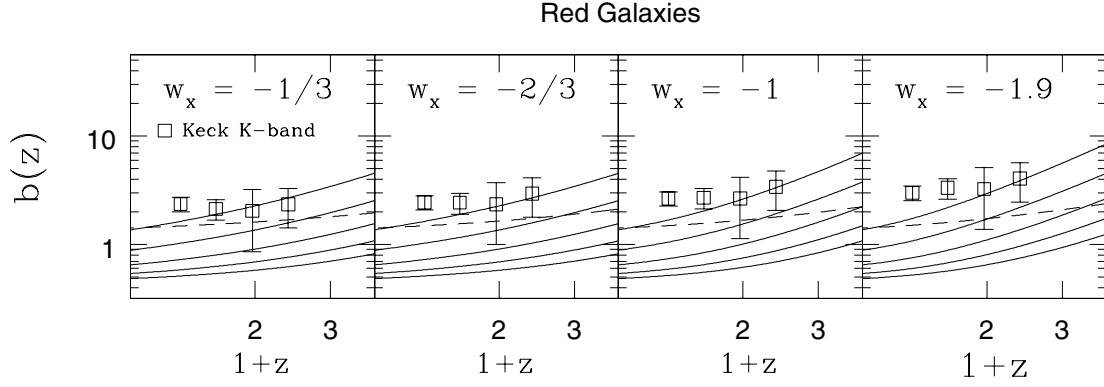


**Figure 2.** Analytical computations of the bias parameters for various quintessence models. Dashed lines are the results from the test-particle model and solid lines represent computations from the halo model. We use the analytical results of Mo & White (1996) to compute bias for haloes larger than a given mass. Curves from the bottom upwards correspond to haloes with masses greater than  $10^9$ ,  $10^{10}$ ,  $10^{11}$ ,  $10^{12}$  and  $10^{13} M_\odot$ . For the test-particle model, we have computed the bias assuming  $\sigma_8 = 1.13$ , as derived from the Stromlo-APM survey (Loveday, Tresse & Maddox 1999) for galaxies with no emission lines (red objects). These bias parameters are computed from the estimated  $r_0$  from these surveys by Magliocchetti et al. (2000). Note that the bias computed from the Mo & White (1996) formalism is not forced to reproduce any observational data. Observational data points correspond to the Keck-K-band survey (Carlberg et al. 1997). See text for more details.

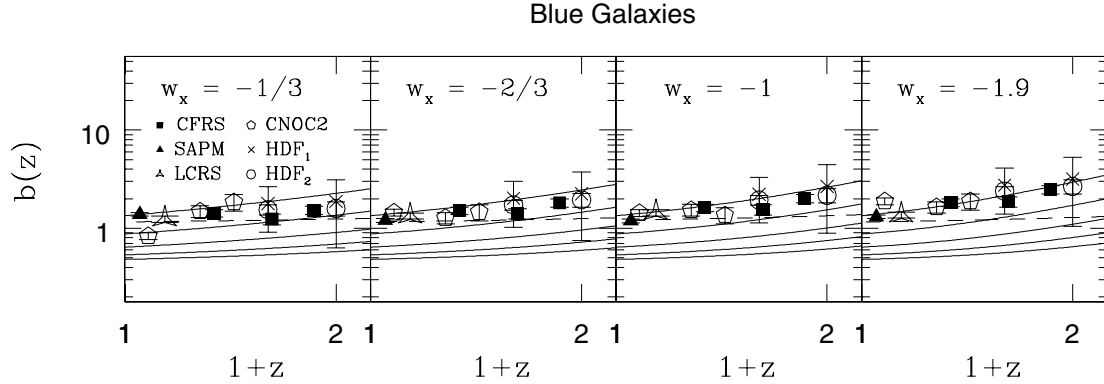


**Figure 3.** As in Fig. 2 but for blue galaxies. In this case, for the test-particle model we have computed the evolution of the bias parameter assuming  $\sigma_8 = 0.93$ , as derived for galaxies with weak emission lines in the Stromlo-APM survey (Loveday et al. 1999). The data points correspond to the following surveys: Canada-France Redshift Survey (CFRS; Le Fevre et al. 1996), Stromlo-APM (Loveday et al. 1995), Las Campanas Redshift Survey (LCRS; Huan et al. 1996), Canadian Network for Observational Cosmology 2 (CNOC2; Carlberg et al. 1997), HDF<sub>1</sub> (Connolly, Szalay & Brummer 1998 and HDF<sub>2</sub> (Magliocchetti & Maddox 1999). See the main text for more details.

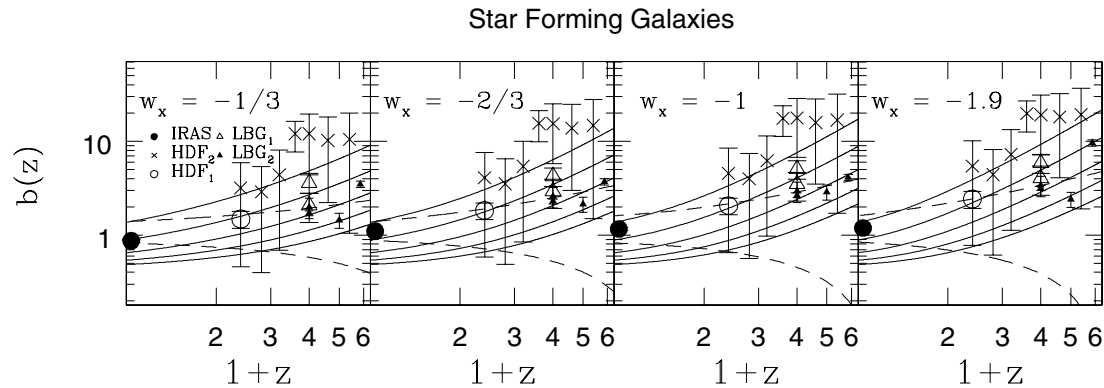


**Figure 4.** As in Fig. 2 but for star-forming galaxies. In this case, we show two different evolutionary tracks for the bias parameter in the test-particle model. The lower one is computed assuming  $\sigma_8 = 0.66$  as derived from galaxies with very strong emission lines (also classified as star-forming galaxies) in the Stromlo-APM survey (Loveday et al. 1999), while the upper one matches the clustering of LBG at redshift 3. Observational data points correspond to the following surveys: IRAS (Saunders, Rowan-Robinson & Lawrence 1992), HDF<sub>1</sub> (Connolly et al. 1998), HDF<sub>2</sub> (Magliocchetti & Maddox 1999), LBG<sub>1</sub> (Giavalisco et al. 1998; Adelberger et al. 1998) and LBG<sub>2</sub> (Porciani & Giavalisco 2002; Adelberger et al. 2003; Ouchi et al. 2001, 2003). See the text for more details.

### 3.2 Press–Schechter and halo bias

In order to compute the evolution of galaxy clustering, it is often convenient to associate galaxies with their host dark matter haloes. This can be done in many different ways; see, for example, Cooray & Sheth (2002) for a recent review. In this paper, for simplicity, we will always assume that a given class of cosmic objects corresponds to a halo population with a mass that is above a given threshold value. The underlying idea is that, at large separations, the correlation function will be dominated by objects residing in different haloes and will be similar to the halo correlation function. The two-point correlation function of dark matter haloes has been the subject of many recent analytical as well as numerical studies. In particular, the use of the peak-background split method (Efstathiou et al. 1988; Cole & Kaiser 1989) and the extended Press–Schechter (see for example, White 2002 for a recent review on Press–Schechter mass function and related issues) formalism have been combined to compute the correlation function of dark matter haloes in Lagrangian space and mapping from Lagrangian space to Eulerian space within the context of spherical collapse model (see Catelan et al. 1998 for a more general approach). Mo & White (1996) have derived an analytical expression (expected to be valid in the large separation limit) for the halo–halo correlation:

$$\xi_{hh}(r; M) = b^2(M) \xi_{mm}(r). \quad (6)$$

Here the bias parameter  $b(M)$  as computed from the Press–Schechter formalism can be written as

$$b(M) = 1 + \frac{\delta_c}{\sigma^2(M)} - \frac{1}{\delta_c}, \quad (7)$$

where  $\sigma(M)$  is the linearly evolved rms density fluctuation of top-hat spheres containing an average mass  $M$ . The parameter  $\delta_c$  is derived from the dynamics of the spherical collapse in an expanding background. It has been shown that the parameter  $\delta_c$  is largely insensitive to background dynamics of the universe (Weinberg & Kamionkowski 2002). In our studies we have fixed  $\delta_c \simeq 1.69$ , which is of sufficient accuracy for our purpose.

Many refinements of the Mo–White calculations can be found in the literature. Catelan et al. (1998) followed the non-linear evolution of the clustering of dark matter haloes using a stochastic approach to biasing. Jing (1998, 1999) and Porciani, Catelan & Lacey (1999) have shown that an improved model for halo selection in Lagrangian space, based on sounder theoretical grounds than the naive Press–Schechter approach, is required to accurately reproduce the outcome of numerical simulations. Sheth et al. (2001) have generalized the formalism by using anisotropic collapse scenarios instead of spherical collapse. This model has been calibrated against  $N$ -body simulations in the  $\Lambda$ CDM cosmology.

It is also possible to construct bias models assuming the hierarchical nature of higher-order correlation functions in gravitational clustering (Bernardeau & Schaeffer 1999). The general trend in such calculations is largely in agreement with halo models (Valageas, Silk & Schaeffer 2001). We plan to discuss such models and their relevance in weak lensing surveys or their cross-correlations with galaxy surveys in future publications.

We have coupled the Press–Schechter formalism with the model of Mo & White (1996) to compute the number densities (Fig. 5) and bias associated with various objects in quintessence cosmologies (Figs 2–4). In order to compare theory and observations, we assume that a given galaxy population corresponds to observing all haloes beyond a certain threshold or cut-off mass  $M_{\min}$ . The corresponding clustering properties are then computed by weighting the bias parameter of haloes of mass  $M$  with the appropriate number

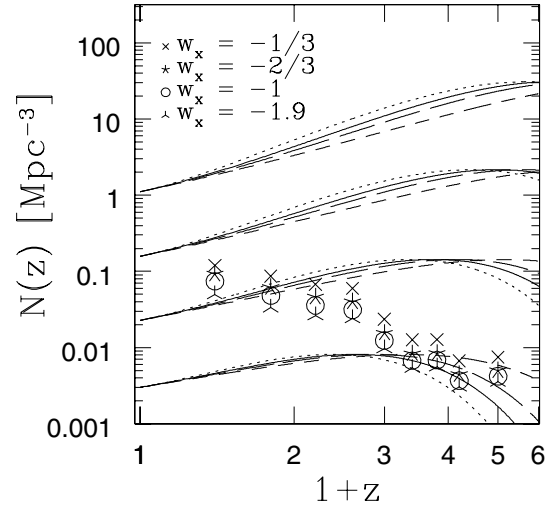


**Figure 5.** The number density of haloes for various quintessence models is plotted as a function of redshift  $z$ . The different sets of curves correspond to haloes with masses greater than  $10^9$ ,  $10^{10}$ ,  $10^{11}$  and  $10^{12} M_{\odot}$  from top to bottom. Different line styles correspond to different values of  $w_X$ . The solid line represents the  $\Lambda$ CDM model. The observational data points come from the HDF analysis (Magliocchetti & Maddox 1999). Note that  $M_{\min}$  inferred from galaxy clustering is consistent with their abundance at high redshift. The data points correspond to the observed number density by assuming a specific equation of state. For a given redshift, the points correspond to decreasing  $w_X$  from top to bottom.

density. Figs 2–4 show the bias parameter for objects heavier than  $10^9$ – $10^{13} M_{\odot}$ . The corresponding values for  $\sigma_8$  are also plotted in Fig. 1 (dotted lines). Our results show a basic degeneracy between the dark energy equation of state and the way galaxies populate dark matter haloes. Typically we find that objects are more biased, and thus correspond to more massive haloes, in cosmologies with more negative values of  $w_X$ . Hopefully, future surveys will reduce the scatter and the uncertainties of the data points. Connecting different populations at different redshifts and understanding the evolution of the corresponding bias parameters will be crucial to inferring constraints on dark energy. On the other hand, the degeneracy between cosmology and galaxy biasing means that pinning down the biasing scheme may not be easy until we better understand the properties of dark energy.

Fig. 5 shows the number density of haloes as a function of redshift for various quintessence models versus data points converted to each model from the *Hubble Deep Field* (HDF) analysis data of Magliocchetti & Maddox (1999). The different sets of curves correspond to haloes with masses greater than  $10^9$ ,  $10^{10}$ ,  $10^{11}$  and  $10^{12} M_{\odot}$  from top to bottom. Different line styles correspond to different values of  $w_X$ . The solid line represents the  $\Lambda$ CDM model. For a given redshift, the data points correspond to decreasing  $w_X$  from top to bottom. The shape of the theoretical curves is typical of any hierarchical scenario for structure formation deriving from primordial Gaussian fluctuations. At early epochs, the halo number density within a given mass interval ( $M > M_{\min}$ ) increases with time as density peaks of lower and lower amplitude go non-linear on the mass scales  $M_{\min}$ . The number density then reaches a maximum at the epoch in which the characteristic mass of the existing haloes coincides with  $M_{\min}$ , and declines afterwards when objects in the interesting mass interval merge to form bigger haloes. Note that  $M_{\min}$  inferred from galaxy clustering is consistent with their abundance at high redshift, suggesting that our simple biasing scheme is accurate

enough to describe the basic properties of galaxy clustering. In fact, it is not surprising that no analytical curve traces the evolution of HDF galaxies because selection effects will pick up totally different populations (probably residing in haloes with different masses) at low and high  $z$ . Hopefully joint analyses of the evolution of the number density and bias parameter of different galaxy populations will help shed some light on the viable cosmological models and biasing schemes.

#### 4 ABUNDANCE AND SPATIAL DISTRIBUTION OF GALAXY CLUSTERS

The abundance of rich clusters as a function of redshift is a promising tool to distinguish cosmological models (Wang & Steinhardt 1998; Mainini & Macciò 2002). The key idea is to constrain the amplitude of the power spectrum of density fluctuations at intermediate redshifts.

In Fig. 6 we plot the evolution of the number density of cluster mass haloes obtained through the Press–Schechter model. It is clear that measuring the cluster abundance at  $z \gtrsim 1$  could potentially distinguish among different dark energy models. This can be done by combining cluster data with other observations which strongly constrain other cosmological parameters such as, for instance, the matter density parameter and the shape of the linear power spectrum of density fluctuations. A simultaneous analysis of the large-scale clustering and the mean abundance of galaxy clusters would give

tighter constraint on the cosmology (e.g. Schuecker et al. 2003a). In Fig. 7 we show how the linear bias of galaxy clusters is expected to evolve with redshift in different dark energy models. As expected in bottom-up scenarios, rarer objects correspond to a stronger clustering amplitude. Clearly, the abundance and spatial distribution of galaxy clusters are a sensitive probe of dark energy at intermediate redshifts.

From the observational point of view, the quest for clusters at intermediate redshifts is becoming a mature field. Deep optical and near-infrared surveys (which look for local galaxy density enhancements) allow the detection of the richest clusters at  $z \sim 1$ . Even though spurious detections and selection effects represent serious problems, these studies will start being suitable for clustering studies as they cover areas in excess of  $100 \text{ deg}^2$ , e.g. the Red-Sequence Cluster Survey (Gladders & Yee 2000) and the Las Campanas Distant Cluster Survey (Nelson et al. 2002).

Alternatively, clusters can be detected in X-rays through the thermal bremsstrahlung emission from the hot intracluster plasma. Selection effects in these samples are much easier to handle with respect to optical surveys. A number of *ROSAT* surveys easily detected galaxy clusters out to redshifts of  $z \sim 0.4$  (Ebeling et al. 1996, 1998, 2000; de Grandi et al. 1999; Böhringer et al. 2000). The upcoming *XMM* Large-Scale Structure Survey (Pierre 2000) will provide about 900 clusters out to a redshift of about 1. This can provide useful constraints on cosmological parameters (assuming a tight control on various systematics; see, for example, Refregier

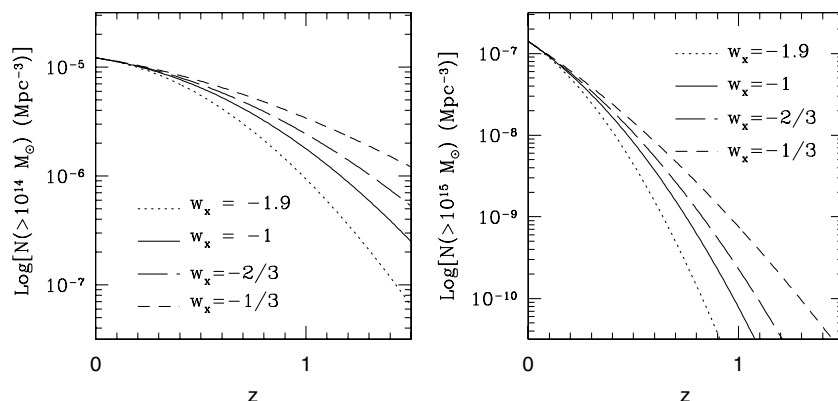


**Figure 6.** The number density of cluster-sized haloes is plotted as a function of redshift  $z$  for various quintessence models. Different curves correspond to different values of the equation of state parameter  $w_x$ . The left panel corresponds to haloes of mass larger than  $10^{14} M_\odot$  and the right panel corresponds to mass greater than  $10^{15} M_\odot$ .

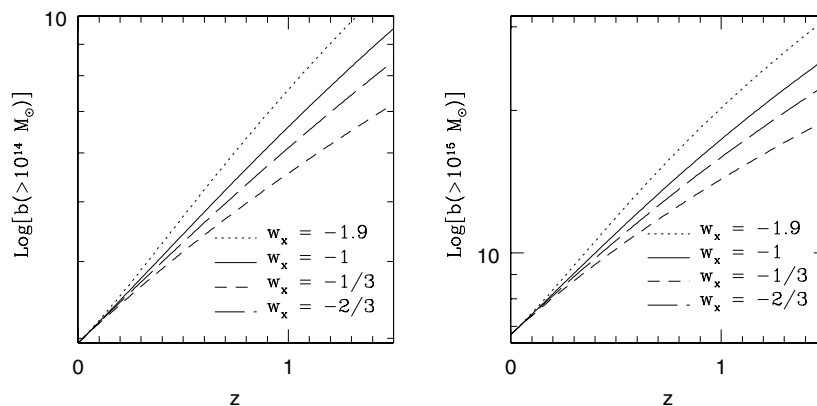


**Figure 7.** As in Fig. 6 but for the bias parameter of cluster-sized haloes.

et al. 2002a, b)). Such surveys with uniform sensitivity will provide a very useful observational data base to constrain both the number density and the bias associated with galaxy clusters (see also Moscardini et al. 2002). Deep multicolour follow-up programmes can identify and measure the redshift of clusters within the range of  $0 < z < 1$ , and near-infrared observations can supplement distant cluster candidates at  $z > 1$ . Cluster two-point statistics can be used to lift the degeneracies involved with estimating the cosmological parameters by using cluster counts alone. Schuecker et al. (2003b) performed a detailed analysis of 452 X-ray brightest clusters mainly for  $z < 0.3$ . Cosmological parameter estimation using the abundance of *ROSAT*–European Southern Observatory Flux-Limited X-Ray (REFLEX) clusters and Type Ia supernovae (SNe Ia) data can produce powerful constraints on the equation of state. Such studies should be supplemented by observations of clustering of galaxy clusters to enhance their sensitivity to the equation of state.

The Sunyaev–Zel’dovich (SZ) effect, e.g. the upscattering of CMB photons by electrons in the hot intracluster medium, is another powerful method to detect high-redshift clusters. For instance, the Massive Cluster Survey (MACS) has already detected eight clusters at  $z > 0.5$  (La Roque et al. 2003). A number of future surveys are expected to detect galaxy clusters exploiting the SZ effect (see, for example, Weller, Battye & Kneissl 2002; Hu 2003). Such studies will conduct deep and narrow surveys using interferometric arrays such as, for example, the Arc-Minute Micro-Kelvin Imager (AMI; Kneissl et al. 2001), the SZ Array (SZA; Carlstrom et al. 2000) or the Array for Microwave Background Anisotropy (AMiBa; Lo et al. 2000). Shallower surveys such as the One Centimeter Receiver Array (OCRA; Browne et al. 2000) will also be useful for their wider sky coverage. The shallow but nearly all-sky survey conducted by *Planck* (whose multifrequency maps will be used for component analysis) will be released to the scientific community and can provide a wealth of information in this direction. For a detailed analysis of the clustering properties of galaxy clusters detectable by *Planck*, see Moscardini et al. (2002). In addition, deep and wide field surveys using 1000-element bolometric arrays mounted on a telescope at the South Pole represent other interesting options for cluster surveys. A more rigorous Fisher matrix analysis of errors associated with such surveys in estimating various cosmological parameters and their cross-correlations will be presented elsewhere.

## 5 DISCUSSION

Today we have a concordance that the Universe is accelerating, its energy dominated by dark energy with a strongly negative equation of state. However, we know almost nothing of the dark energy – its equation of state  $w_X$  or whether this evolves. These two quantities hold crucial clues to the underlying fundamental physics. Therefore, by mapping the expansion history of the Universe we can probe the new physics. Future distance–redshift observations of SNe Ia (Wang 2000; Supernova/Acceleration Probe<sup>2</sup>) should place useful constraints on the dark energy density (Wang & Garnavich 2001; Wang & Lovelace 2001; Wang et al. 2003). If these constraints are consistent with a quintessence model, then we can hope to map the potential associated with the scalar field using complementary data, including that of galaxy clustering. Several new experiments are being carefully designed to probe the dark energy. Systematic uncertainties rather than merely paucity or imprecision of observations will be the key obstacle; this underscores the critical importance

of using independent and complementary methods to probe dark energy.

In this paper we have concentrated on the effect of the equation of state on galaxy clustering. We find that galaxies are more biased (thus corresponding to more massive haloes) in models with more negative values of dark energy equation of state  $w_X$ . Results from various galaxy surveys are corrected of systematic biases and used to compare against quintessence models. We have shown that correcting the scale dependence of galaxy clustering does reduce the observed scatter in estimated bias among various data sets, at least for moderately high redshifts. In spite of this, current data from galaxy clustering do not place strong constraints on quintessence models (see Figs 1–4), primarily due to the inhomogeneity of the data (consisting of many different surveys) and the small area covered by each survey. However, our results clearly show the potential of future homogeneous, deep, and wide-field surveys in constraining dark energy models. In particular, we have shown that the abundance and spatial distribution of galaxy clusters from such surveys are strongly dependent on the dark energy equation of state at intermediate redshifts (see Figs 6 and 7). In future publications, we will study the quantitative constraints on dark energy that can be derived from future homogeneous, deep, and wide-field galaxy surveys.

The study of the dynamics of the quintessence field directly from observations would provide an interesting new independent window to high-energy physics. As proposed by Starobinsky (1998), luminosity–distance measurements of SNe Ia provide such a possibility. Similarly, the observed evolution of clustering of galaxies at various redshifts can be used to construct the potential  $V(\phi)$  associated with the dark energy scalar field  $\phi$ . In principle, we need to relate the evolution of  $H(z)$  from the observed evolution of the mass density contrast  $\delta$  (Starobinsky 1998)

$$\frac{H^2(z)}{H^2(0)} = \frac{(1+z)^2 \delta^2(0)}{\delta^2(z)} - 3\Omega_m \frac{(1+z)^2}{\delta^2(z)} \int_0^z \frac{\delta(z)|\delta'(z)|}{1+z} dz, \quad (8)$$

where primes denote derivative with respect to the redshift  $z$ .<sup>3</sup> On large scales, we expect that  $\delta$  and fluctuations in the number density distribution of galaxies,  $\delta_g$ , are related by some bias factor as described above  $\delta_g(z) = b(z)\delta(z)$ . Once galaxy biasing has been specified, next we need to relate the evolution of the Hubble parameter  $H(z)$  to the potential of the scalar field  $V(\phi)$  (Saini et al. 2000):

$$\frac{8\pi G}{3H_0^2} V(\phi) = \frac{H^2(z)}{H_0^2} - \frac{(1+z)}{6H_0^2} \frac{dH^2(z)}{dz} - \frac{1}{2} \Omega_m (1+z)^3 \quad (9)$$

$$\frac{8\pi G}{3H_0^2} \left( \frac{d\phi}{dz} \right)^2 = \frac{2}{3H_0^2(1+z)} \frac{d \ln H}{dz} - \frac{\Omega_m(1+z)}{H^2}. \quad (10)$$

As pointed out before, a simplistic linear-biasing picture may not be correct as we will need a more complete picture of the physics associated with the galaxy formation process. In this paper, we have explored a number of analytical models of galaxy bias. Even though they look plausible when compared to present data, a cleaner methodology will probably be required to reconstruct the scalar field potential directly from galaxy clustering. Future weak lensing surveys will be very useful in this respect and cross-correlating weak lensing surveys with redshift surveys will provide us with a direct handle on  $b(z)$ , which in turn will be used to reconstruct the scalar

<sup>2</sup> <http://snap.lbl.gov/>

<sup>3</sup> This applies to the linear regime, and corrections are required on smaller scales.



field potential  $V(\phi)$ . However, the toy models that we have studied in this paper can provide a valuable starting point.

In summary, at present it is not realistic to place strong constraints on dark energy from observed galaxy clustering. However, future generation surveys with much higher sky coverage, when complemented by detailed measurements of evolution of gravitational clustering from weak lensing measurements, will provide direct constraints on evolution of linear growth of density perturbations. These, combined with the constraints of the dark energy density from future supernova data (Wang & Garnavich 2001; Wang & Lovelace 2001; Wang et al. 2003), will make it possible not only to constrain but perhaps even to reconstruct the potential associated with the scalar field  $\phi$ .

## ACKNOWLEDGMENTS

DM acknowledges support from the Particle Physics and Astronomy Research Council (PPARC) by grant RG28936. CP has been partially supported by the Zwicky Prize Fellowship programme at ETH-Zürich and by the European Research and Training Network ‘The Physics of the Intergalactic Medium’. YW acknowledges support from National Science Foundation (NSF) CAREER grant AST-0094335. We are grateful to Manuela Magliocchetti for sharing with us the published data points from various galaxy surveys, and for helpful discussions. It is a pleasure for DM to acknowledge many fruitful discussions with members of the Cambridge Leverhulme Quantitative Cosmology Group.

## REFERENCES

- Adelberger K. L., Steidel C. C., Giavalisco M., Dickinson M., Pettini M., Kellogg M., 1998, *ApJ*, 505, 18
- Adelberger K. L., Steidel C. C., Shapley A. E., Pettini M., 2003, *ApJ*, 584, 45
- Barger V., Marfatia D., 2001, *Phys. Lett. B*, 498, 67
- Bassett B. A., Kunz M., Silk J., Ungarelli C., 2002, *MNRAS*, 336, 1217
- Bean R., Melchiorri A., 2002, *Phys. Rev. D*, 65, 041302
- Benabed K., Bernardeau F., 2001, *Phys. Rev. D*, 64, 083501
- Bernardeau F., Schaeffer R., 1999, *A&A*, 349, 697
- Bernardeau F., Colombi S., Gaztanaga E., Scoccimarro R., 2002, *Phys. Rep.*, 367, 1
- Böhringer H. et al., 2000, *ApJS*, 129, 435
- Browne I. W., Wilkinson P. N., Mao S., Davis R., Roddis N., 2000, in Butcher H. R., ed, *Radio Telescopes. Proc. SPIE*, 4015, 33
- Budavári T., Szalay A. S., Connolly A. J., Csabai I., Dickinson M., 2000, *AJ*, 120, 1588
- Caldwell R. R., 2002, *Phys. Lett. B*, 545, 23
- Caldwell R. R., Dave R., Steinhardt P. J., 1998, *Phys. Rev. Lett.*, 80, 1582
- Carlberg R. G. et al., 1997, *ApJ*, 484, 538
- Carlstrom J. E. et al., 2000, in Durret F., Gerbal G., eds, *Constructing the Universe with Clusters of Galaxies*, Paris, France
- Catelan P., Lucchin F., Matarrese S., Porciani C., 1998, *MNRAS*, 297, 692
- Cole S., Kaiser N., 1989, *MNRAS*, 237, 1127
- Coles P., Melott A. L., Munshi D., 1999, *ApJ*, 521, L5
- Colombi S., Bouchet F. R., Schaeffer R., 1995, *ApJS*, 96, 401
- Colombi S., Bernardeau F., Bouchet F. R., Hernquist L., 1997, *MNRAS*, 287, 241
- Connolly A. J., Szalay A. S., Brummer R. J., 1998, *ApJ*, 499, L125
- Cooray A. R., Sheth R., 2002, *Phys. Rep.*, 372, 1
- Davis M., Peebles P. J. E., 1977, *ApJS*, 34, 425
- de Grandi S. et al., 1999, *ApJ*, 514, 148
- Dekel A., 1986, *Comments Astrophys.*, 11, 235
- Dekel A., Lahav O., 1999, *ApJ*, 520, 24
- Dekel A., Rees M. J., 1987, *Nat*, 326, 455
- Ebeling H., Voges W., Böhringer H., Edge A. C., Huchra J. P., Briel U. G., 1996, *MNRAS*, 281, 799
- Ebeling H., Edge A. C., Böhringer H., Allen S. W., Crawford C. S., Fabian A. C., Voges W., Huchra J. P., 1998, *MNRAS*, 301, 881
- Ebeling H., Edge A. C., Allen S. W., Crawford C. S., Fabian A. C., Huchra J. P., 2000, *MNRAS*, 318, 333
- Efstathiou G., 1999, *MNRAS*, 310, 842
- Efstathiou G., Frenk C. S., White S. D. M., Davis M., 1988, *MNRAS*, 235, 715
- Fernández-Soto A., Lanzetta K. M., Chen H., Pascarelle S. M., Yahata N., 2001, *ApJS*, 135, 41
- Frampton P. H., 2003, *Phys. Lett. B*, 555, 139
- Freese K., Adams F. C., Frieman J. A., Mottola E., 1987, *Nucl. Phys. B*, 287, 797
- Frieman J. A., Hill C. T., Stebbins A., Waga I., 1995, *Phys. Rev. Lett.*, 75, 2077
- Fry J. N., 1986, *ApJ*, 308, L71
- Fry J. N., Peebles P. J. E., 1978, *ApJ*, 221, 19
- Garnavich P. M. et al., 1998a, *ApJ*, 493, L53
- Garnavich P. M. et al., 1998b, *ApJ*, 509, 74
- Giavalisco M., Steidel C. C., Adelberger K. L., Dickinson M. E., Pettini M., Kellogg M., 1998, *ApJ*, 503, 543
- Gladders M. D., Yee H. K. C., 2000, *AJ*, 120, 2148
- Groth E., Peebles P. J. E., 1977, *ApJ*, 217, 385
- Hamilton A. J. S., Kumar P., Lu E., Matthews A., 1991, *ApJ*, 374, L1
- Heath D. J., 1977, *MNRAS*, 179, 351
- Hu W., 2003, *Phys. Rev. D*, 67, 081304
- Huan L., Kirshner R. P., Shtetman S. A., Landy S. D., Oemler A., Tucker D. L., Schechter P. L., 1996, *ApJ*, 471, 617
- Huterer D., Turner M. S., 2001, *Phys. Rev. D*, 64, 123527
- Jain B., Seljak U., 1997, *ApJ*, 484, 560
- Jain B., van Waerbeke L., 2000, *ApJ*, 530, L1
- Jain B., Mo H. J., White S. D. M., 1995, *MNRAS*, 276, L25
- Jenkins A. et al., 1998, *ApJ*, 499, 20
- Jing Y. P., 1998, *ApJ*, 503, L9
- Jing Y. P., 1999, *ApJ*, 515, L45
- Kaiser N., 1992, *ApJ*, 388, 272
- Kaiser N., 1998, *ApJ*, 498, 26
- Kneissl R., Jones M. E., Saunders R., Eke V. R., Lasenby A. N., Grainge K., Cotter G., 2001, *MNRAS*, 328, 783
- Kujat J., Linn A. M., Scherrer R. J., Weinberg D. H., 2002, *ApJ*, 572, 1
- Lahav O., Rees M. J., Lilje P. B., Primack J. R., 1991, *MNRAS*, 251, 128
- La Roque S. J. et al., 2003, *ApJ*, 583, 559
- Le Fevre O., Hudon D., Lilly S. J., Crampton David, Hammer F., Tresse L., 1996, *ApJ*, 461, 534
- Lo K. Y., Chiueh T., Liang H., Ma C. P., Martin R., Ng K.-W., Pen U. L., Subramanian R., 2000, in Lasenby A., Wilkinson A., eds, *New Cosmological Data and the Values of the Fundamental Parameters*, International Astronomical Union Symposium no. 201
- Loveday J., Maddox S. J., Efstathiou G., Peterson B. A., 1995, *ApJ*, 442, 457
- Loveday J., Tresse L., Maddox S. J., 1999, *MNRAS*, 310, 281
- Lowenthal J. D. et al., 1997, *ApJ*, 481, 673
- Ma C., Caldwell R. R., Bode P., Wang L., 1999, *ApJ*, 521, L1
- Madau P., Ferguson H. C., Dickinson M. E., Giavalisco M., Steidel C. C., Fruchter A., 1996, *MNRAS*, 283, 1388
- Magliocchetti M., Maddox S. J., 1999, *MNRAS*, 306, 988
- Magliocchetti M., Porciani C., 2003, *MNRAS*, 346, 186
- Magliocchetti M., Bagla J. S., Maddox S. J., Lahav O., 2000, *MNRAS*, 314, 546
- Mainini R., Macciò A. V., 2002, *NewA*, 8, 173
- Maoli R., Van Waerbeke L., Mellier Y., Schneider P., Jain B., Bernardeau F., Erben T., Fort B., 2001, *A&A*, 368, 766
- Maor I., Brustein R., Steinhardt P. J., 2001, *Phys. Rev. Lett.*, 86, 6 (erratum *Phys. Rev. Lett.*, 87, 049901)
- Maor I., Brustein R., McMahon J., Steinhardt P. J., 2002, *Phys. Rev. D*, 65, 123003

Matarrese S., Coles P., Lucchin F., Moscardini L., 1997, MNRAS, 286, 115

Metcalfe R. B., Silk J., 1999, ApJ, 519, L1

Mo H. J., White S. D. M., 1996, MNRAS, 282, 347

Moscardini L., Bartelmann M., Matarrese S., Andreani P., 2002, MNRAS, 335, 984

Munshi D., Wang Y., 2003, ApJ, 583, 566

Nelson A. E., Gonzalez A. H., Zaritsky D., Dalcanton J. J., 2002, ApJ, 566, 103

Ng S. C. C., Wiltshire D. L., 2001, Phys. Rev. D, 64, 123519

Nusser A., Davis M., 1994, ApJ, 421, L1

Onemli V. K., Woodard R. P., 2002, Class. Quantum Grav., 19, 4607

Ouchi M. et al., 2001, ApJ, 558, 83

Ouchi M. et al., 2003, ApJ, 582, 60

Padmanabhan T., 2003, Phys. Rep., 380, 235

Peacock J. A., Dodds S. J., 1996, MNRAS, 280, L19

Peebles P. J. E., Ratna B., 1988, ApJ, 325, L17

Perlmuter S. et al., 1999, ApJ, 517, 565

Pierre M., 2000, preprint(astro-ph/0011166)

Podariu S., Ratna B., 2000, ApJ, 532, 109

Podariu S., Nugent P., Ratna B., 2001, ApJ, 553, 39

Porciani C., Giavalisco M., 2002, ApJ, 565, 24

Porciani C., Matarrese S., Lucchin F., Catelan P., 1998, MNRAS, 298, 1097

Porciani C., Catelan P., Lacey C., 1999, ApJ, 513, L99

Refregier A., Rhode J., Groth E., 2002a, ApJ, 572, L131

Refregier A., Valtchanov I., Pierre M., 2002b, A&A, 390, 1

Rhode J., Refregier A., Groth E., 2001, ApJ, 552, L85

Riess A. G. et al., 1998, AJ, 116, 1009

Sahni V., Starobinsky A., 2000, Int. J. Mod. Phys. D, 9, 373

Sahni V., Wang L., 2000, Phys. Rev. D, 62, 103517

Saini T. D., Raychaudhury S., Sahni V., Starobinsky A. A., 2000, Phys. Rev. Lett., 85, 1162

Sarbu N., Rusin D., Ma C., 2001, ApJ, 561, L147

Saunders W., Rowan-Robinson M., Lawrence A., 1992, MNRAS, 258, 134

Schuecker P., Böhringer H., Collins C. A., Guzzo L., 2003a, A&A, 398, 867

Schuecker P., Caldwell R. R., Böhringer H., Collins C. A., Guzzo L., 2003b, A&A, 402, 53

Scoccimarro R., Frieman J. A., 1999, ApJ, 520, 35

Seljak U., Holz D. E., 1999, A&A, 351, L10

Sheth R. K., Tormen G., 1999, MNRAS, 308, 119

Sheth R. K., Mo H. J., Tormen G., 2001, MNRAS, 323, 1

Smith R. E. et al., 2003, MNRAS, 341, 1311

Starobinsky A. A., 1998, in Mueller V., Gottloeber S., Muecket J. P., Wambsgans J., eds, Large Scale Structure: Tracks and Traces. Proceedings of the 12th Potsdam Cosmology Workshop, Potsdam, 15–19 September 1997. World Scientific, Singapore, pp. 375–380

Steidel C. C., Giavalisco M., Pettini M., Dickinson M., Adelberger K. L., 1996, ApJ, 462, L17

Steidel C. C., Adelberger K. L., Dickinson M., Giavalisco M., Pettini M., Kellogg M., 1998, ApJ, 492, 428

Steinhardt P. J., Wang L., Zlatev I., 1999, Phys. Rev. D, 59, 123504

Szapudi I., Szalay A. S., 1993, ApJ, 408, 43

Valageas P., Silk J., Schaeffer R., 2001, A&A, 366, 363

Waga I., Frieman J. A., 2000, Phys. Rev. D, 62, 043521

Wald R. M., 1984, General Relativity, The University of Chicago Press, Chicago

Wang Y., 1999, ApJ, 525, 651

Wang Y., 2000, ApJ, 531, 676

Wang Y., Garnavich P., 2001, ApJ, 552, 445

Wang Y., Lovelace G., 2001, ApJ, 562, L115

Wang L., Steinhardt P. J., 1998, ApJ, 508, 483

Wang Y., Bahcall N., Turner E. L., 1998, AJ, 116, 2081

Wang Y., Holz D. E., Munshi D., 2002, ApJ, 572, L15

Wang Y., Freese K., Gondolo P., Lewis M., 2003, ApJ, 594, 25

Weinberg N., Kamionkowski M., 2002, MNRAS, 337, 1269

Weller J., Albrecht A., 2002, Phys. Rev. D, 65, 103512

Weller J., Battye R., Kneissl R., 2002, Phys. Rev. Lett., 88, 231301

White M., 1998, ApJ, 506, 495

White M., 2002, ApJS, 143, 241

Wilson G., Kaiser N., Luppino G. A., 2001, ApJ, 556, 601

Wittman D. M., Tyson J. A., Kirkman D., Dell’Antonio I., Bernstein G., 2000, Nat, 405, 143

## APPENDIX A: CONVERTING OBSERVATIONAL DATA FOR VARIOUS COSMOLOGIES

We assume a power-law form for the two-point correlation function,  $\xi(r, z) = [r/r_0(z)]^{-\gamma}$ .<sup>4</sup> The transformation among various cosmological models can be derived by requiring that the angular correlation function for a given set of galaxies is the same in different cosmologies. This implies

$$r_{02} = \left[ \frac{h_{01}}{h_{02}} \left( \frac{x_1(z)}{x_2(z)} \right)^{1-\gamma} \frac{E_1(z)}{E_2(z)} \right]^{1/\gamma} r_{01}(z), \quad (\text{A1})$$

where  $E(z)$  is given by

$$E(z) \equiv \sqrt{\Omega_m(1+z)^3 + \Omega_k(1+z)^2 + \Omega_x f(z)} \quad (\text{A2})$$

and  $x(z)$  is the comoving distance at redshift  $z$ . Note that our expression for the transformation of  $r_0$  between different cosmological models is equivalent to, but greatly simplified from, that of Magliocchetti & Maddox (1999) and Magliocchetti et al. (2000).

We have used the expressions given in Magliocchetti et al. (2000 see, for example, equations 5, 6, 8 and 17) to compute  $\sigma_8$  and  $b^2(\bar{r}, z)$ . We write

$$\sigma_8(\bar{r}) = \left\{ \left[ \frac{r_0(\bar{r})}{8} \right]^\gamma c_\gamma \right\}^{1/2}, \quad (\text{A3})$$

$$c_\gamma = \frac{72}{(3-\gamma)(4-\gamma)(6-\gamma)2^\gamma}.$$

The errors on  $r_0$  and  $\gamma$  are propagated into the error of  $\sigma_8$ . The scale-dependent bias is defined as

$$b^2(\bar{r}, z) = \frac{\xi_g(\bar{r}, z)}{\xi_m(\bar{r}, z)}, \quad (\text{A4})$$

where

$$\xi_g(\bar{r}, z) = [\bar{r}/r_0(z)]^{-\gamma},$$

$$\xi_m(\bar{r}, z) = \int \Delta^2(k, z) \frac{\sin k\bar{r}}{k\bar{r}} \frac{dk}{k}, \quad (\text{A5})$$

with  $\Delta^2(k, z)$  denoting the non-linear power spectrum, calculated using the Peacock & Dodds (1996) fitting formulae (normalized to  $\sigma_8^{\text{lin}} = 0.8$  as described above).

For the four new data points we consider (LBG at  $z = 3$ , and Ly  $\alpha$  emitters at  $z = 4.86$ ), we have followed Magliocchetti et al. (2000) in assigning characteristic scales to each survey. We used  $\bar{r} = 5h^{-1}$  Mpc for the  $z = 3$  data point from Adelberger et al. (2003). For the other three new data points, we set the scale  $\bar{r} = \theta_{\text{max}} x(z)$ , and used  $\theta_{\text{max}}$  of 100 arcsec, 16.67 arcmin and 15 arcmin for the data at  $z = 3$  (Porciani & Giavalisco 2002),  $z = 4$  (Ouchi et al. 2001) and  $z = 4.86$  (Ouchi et al. 2003), respectively.

<sup>4</sup> A summary of some observational results for various surveys can be found in (Magliocchetti et al. 2000).